Finite Element Modelling of Flexural Plate Devices

Glenn I. Matthews*[1,2], Samuel J. Ippolito[1,2], Kourosh Kalantar-zadeh[1,2], Wojtek Wlodarski[1,2], and Anthony Holland[1]
[1]School of Electrical and Computer Engineering
RMIT University, Melbourne, AUSTRALIA
*Email: s9806752@student.rmit.edu.au
[2]CRC for microTechnology, Melbourne, AUSTRALIA

***Abstract*— A two dimensional finite element model has been developed for the simulation of a layered flexural plate wave device using the ANSYS package. The simulated device consists of a 2.0 µm silicon nitride thin film, followed by a 0.4 µm aluminum ground layer. A 0.6 µm zinc oxide piezoelectric layer was defined to excite acoustic waves. Good agreement of device frequency response and displacement profiles have been achieved in comparison with other numerical simulation methods. In this paper, the finite element (FE) method is proposed as a benchmark for an alternative analysis based upon a Green's function method. Furthermore, the FE method can be used to obtain other device parameters, such as insertion loss and charge density, which are presented.**

Keywords: Flexural Plate Waves, Lamb, Finite Element, ANSYS

I. INTRODUCTION

Flexural Plate Wave (FPW) devices offer significant advantages over current acoustic sensors when used in liquid sensing applications [1]. A key advantage of the FPW family of devices is their relatively low operating frequency. When used in a liquid phase, the propagating modes of interest are limited to below 10MHz. This operational frequency is mainly restricted due to fabrication limitations. Advantages of working at low frequency include relatively inexpensive signal processing equipment.

Whilst FPW devices are highly sensitive in comparison with other acoustic sensors [2], such as Surface Acoustic Wave (SAW) devices, fabrication still poses significant difficulties. Many different thin films must be successfully deposited to create a single device. Care must also be taken to ensure that metallic films are not compromised during the wet chemical etching of the silicon substrate. By utilising the Finite Element (FE) method, a FPW device can be accurately evaluated before fabrication takes place. This paper presents a FE simulation for a FPW device and the associated difficulties in constructing an accurate model.

II. DEVICE STRUCTURE

Figure 1 depicts the simulated structure. Potential theory [3] shows that the FPW devices mainly support longitudinal and normal displacements. Due to the minimal interaction along the z-direction, a two-dimensional model was considered sufficient. The device consists of a 2.0 µm silicon nitride (Si_3N_4) thin film, followed by a 0.4 µm aluminium (Al) ground layer. Finally a 0.6 µm piezoelectric zinc oxide (ZnO) layer was defined. The total length of the structure was varied to examine the effect on device frequency response. To reduce computational time it was decided to ignore the silicon support structure. Whilst the supports may generate further reflections, this study was primarily concerned with propagation in the plate structure.

The model was constructed with a node density of approximately 1 node every 2.0 µm on the surface. This corresponds to 48 nodes per wavelength. Eleven nodes were distributed throughout the device depth. The ANSYS 'plane13' element, a two-dimensional coupled field structure, was utilised. This element consists of four corner nodes, with support for four degrees of freedom per node [4]. This particular element supports structural, electric and piezoelectric solutions. The magnetic field contribution was ignored for this analysis. Care was taken to ensure that the elements formed were rectangular. For a piezoelectric analysis, the voltage and displacement (UX and UY) degrees of freedom (DOF) were coupled. Material constants were entered in the form of stiffness (c) and piezoelectric matrices (e), permittivity (ε) and density (ρ).

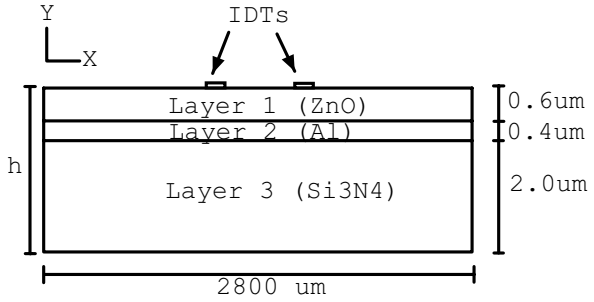

Figure 1. Simplified diagram of FPW device used for FE simulations

Interdigital transducers (IDTs) were modeled by coupling groups of nodes at the ZnO surface to a common voltage [5]. Similarly, the Al ground plane was formed by coupling the nodes in this layer to zero volts. Four IDT fingers, 2 pairs, were defined for both the transmitter and receiver. Edge to edge IDT spacing was 500 µm. Mass loading and reflections caused by the IDTs were excluded for simplicity.

III. SIMULATION PARAMETERS

The transmission matrix method developed by Adler [6], specifies that the simulated device, operating at 4.67 MHz will

have an operational wavelength of approximately 96 μm. This corresponds to a thickness to wavelength ratio (h/λ) of 3×10^{-2}. For this ratio, the first two modes of the device are excited. The anti-symmetrical (A_0) mode propagates along the device with a velocity of 4.47×10^{2} m/s, whilst the symmetrical (S_0) mode propagates at 8.53×10^{3} m/s. As the wavelength at centre frequency is fixed by the period of the IDTs, the A_0 mode theoretically operates at 4.67 MHz, whereas the S_0 wavefront has a centre frequency of approximately 89.1 MHz. Generally, when operated in a liquid phase, the S_0 mode may be dissipated into the surrounding medium, whilst the anti-symmetrical mode will be confined to the device.

IV. Frequency Response

Device frequency response was obtained by performing a two dimensional transient analysis using the ANSYS FE software. The response can be extracted from the FE model by taking the Fourier transform of the voltage on the receiver with respect to time. A 7.45 ns pulse was used to excite the transmitting IDT. The model was then analyzed for a further 299 steps, corresponding to a total simulation time of 2.235 μs. Figure 2 clearly identifies the two wavefronts propagating along the device. The displacements have been scaled to allow for easier identification. The main device frequency response, Figure 3, exhibits a contribution generated by inaccuracies in the modeling. These inaccuracies were caused by reflections in the device boundaries. The first simulation, performed with a device length of 2800 μm, indicates that the S_0 mode reflects before the A_0 wavefront, the mode of interest, has reached the receiving IDT. In practice the S_0 mode could potentially decay into the liquid media, thus its effect would not be as profound.

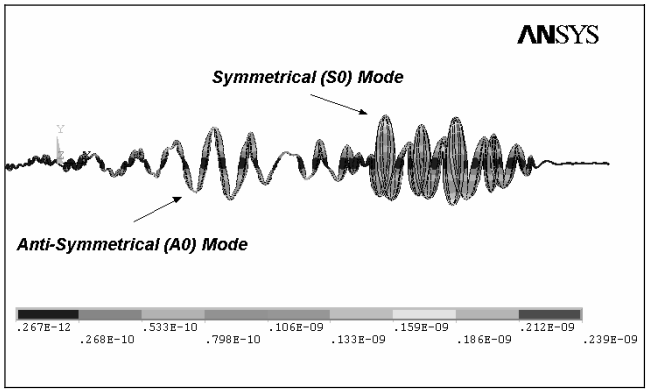

Figure 2. FPW scaled displacement after 130 timesteps.

To obtain the device frequency response, a windowed Fourier Transform of the receiving IDT voltage was undertaken. Figure 3 illustrates the frequency response of the simulated structure. It was found that that the maximum calculated frequency is less than the S_0 operational frequency. This limitation is caused by the size of timesteps used. Further determination of device frequency response can be obtained by selecting a finer timestep, in the order of 3ns. This will allow for a maximum frequency of ~166.67 MHz to be resolved. With a reduction in timestep, the total simulation steps must be increased. It was decided to utilise an 800 step simulation, resulting in a total time of 2.36 μs. Figure 3, demonstrates the effect of increasing the simulation timestep resolution.

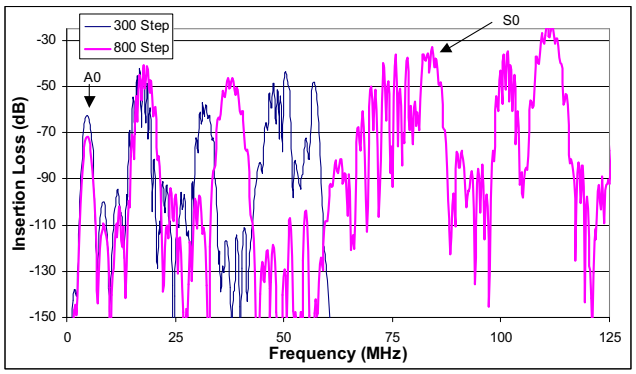

Figure 3. Frequency response for two different timesteps.

Reflections at the device boundaries have the potential to corrupt the true frequency response. To evaluate the variance in results, the model was extended to a total length of 23000 μm. Naturally an increase of almost 10 fold, with the average nodal density the same as previous simulations requires significantly more computational time. However, the extended model has the advantage of minimizing the effect of the reflected S_0 mode reaching the output IDT before the A_0 wavefront passes. Figure 4 provides a comparison between the two different length simulations.

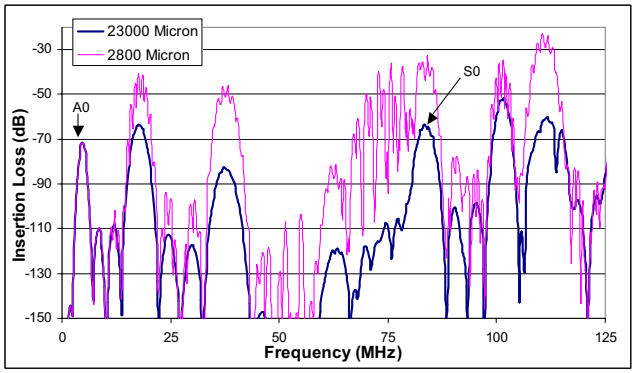

Figure 4. Frequency Response for alternative simulation lengths

Figure 4 indicates that for both models, the two modes of interest have been successfully resolved. Whereas Adler [6] suggets the operating frequency for the S_0 mode is 89.1MHz, ANSYS suggests a frequency of 84.6MHz. The anti-symmetrical mode has been correctly resolved at 4.67MHz. The insertion loss for the A_0 mode is identical despite the changes in simulation length. Of note is the difference in insertion loss for higher order modes. It is believed that the reduction in insertion loss can be attributed by the extension of the model and hence a reduction in acoustic reflections at the device boundaries. For a bidirectional IDT, two wavefronts are always generated. The first travels in the direction of the receiver, whilst the second propagates in the opposite direction. In the 2800 μm structure, the second wavefront reaches the

boundary, reflects and then travels towards the receiving IDT. It is this action that is believed to cause the ripple in the 60-83 MHz region. In a practical device, the reflected wavefront is damped, and hence its effect would not be as profound.

Even though the FE method can be used to generate device parameters such as frequency response, it quite often time consuming and requires a complete description of the surrounding media.

The results from the FE method have been used to verify a more computationally efficient solution based upon a spectral Green's function [7],[8]. Figure 5 depicts the frequency response of the FPW device for both methods. However, it should be noted that the Green's function solution does not take velocity dispersion into account. For a plate mode device and under the frequency range of interest, the result will not vary greatly. Good agreement has been achieved using the Green's function solution.

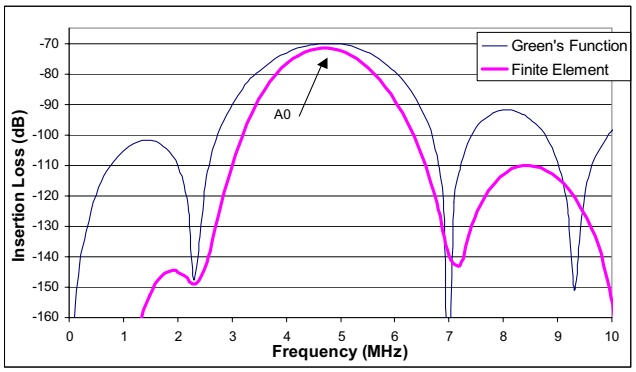

Figure 5. Comparison of FE and Green's Function Frequency Response

V. Electrostatic Analysis

An electrostatic analysis was also performed on the 2800µm device. Whereas a pulse function was applied to generate the frequency response, an electrostatic analysis was performed using a DC voltage of +/- 0.5V on alternative transmitter electrodes. The Al layer was once again forced to ground. The focus of the electrostatic analysis was to determine the charge density on the electrodes and utilise these results to compare against a more computationally efficient method, originally described by Baghai-Wadji et al. [7]. The solution developed by the authors is based upon a Green's function analysis, generating the effective permittivity for a plate device bounded by a ground plane and then using these results to calculate the charge density based on methods in [8] and [9]. Verification of the electrostatic charge density has proven that the alternative method is accurate.

Electrostatic analysis of an IDT indicates that the charge density approaches infinity at the electrode edge. The FE method however assumes that the field variables vary smoothly, thus some error will be associated with the charge at these edges. However, provided that the nodal density is relatively high over the electrode width, then this error should not be significant. A modified form of Simpson's Rule [9] provides an effective workaround for the charge at the electrode edge by dividing the finger into several uneven regions. In the proposed FE model, the node spacing is equal.

Figure 6 depicts the surface charge density with a nodal density of 1 node / 2.0 µm. It can be seen that along the electrode edges, the charge begins to increase, however does not approach infinity. The FE model demonstrates that the charge density changes polarity at the electrode edge. It is believed that this discrepancy is caused by the linear interpolation used in the analysis. If the node density is increased about the electrode edge, this effect is reduced, however not totally negated. As there is no conducting medium between the IDT fingers, the charge in this region should be zero.

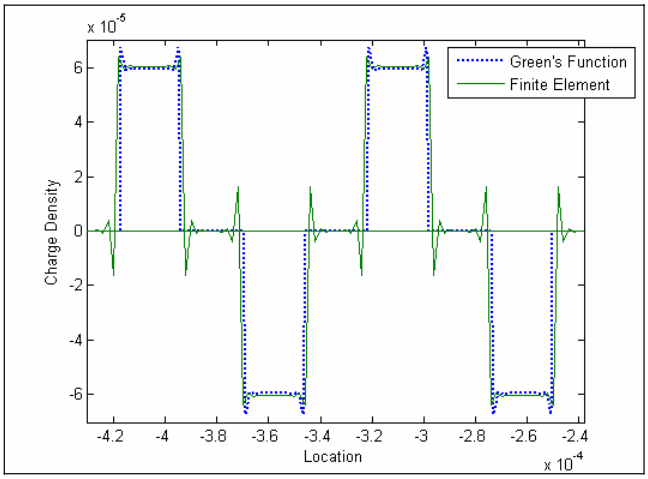

Figure 6. Finite Element Electrostatic Analysis

To perform a comparison between the Green's function and FE solutions, an integral is taken over the device surface. Table 1 demonstrates these results. Whilst increasing the nodal density increases accuracy, consideration must be taken into account of the computational effort required to solve the problem.

TABLE I. Residual Charge vs. Node Density

Node Density	Total Nodes	Residual Charge
1 node / 2.0 um	9807	-2.94E-14
1 node / 1.0 um	19607	1.97E-16
1 node / 0.6 um	29407	2.57E-17
Green's function	52	0.00E+00

Charge neutrality states that the total charge across the device surface must equal zero. Table 1 indicates that despite the previously mentioned issues with the FE method, the electrostatic analysis appears to be converging to the theoretical solution of zero. As the piezoelectric layer is bounded by an Al ground plane, the model can be simplified further by removing the Si_3N_4 and Al ground layers, provided that the backside of the ZnO is grounded. Comparison of original 2800 µm model and the reduced model has proved that this approximation is justified. A reduction in model layers

allows for larger structures to be simulated whilst still maintaining the same node density.

VI. Depth vs. Displacement Profiles

Figure 7 depicts particle displacement profiles that have been obtained using the FE method. The response magnitude has been normalised to that of displacement at the device surface. Identification of modes (A_0 or S_0) is primarily achieved by examining the displacement profile at a given timestep. The results are in good agreement with an alternative method originally derived by Adler [6].

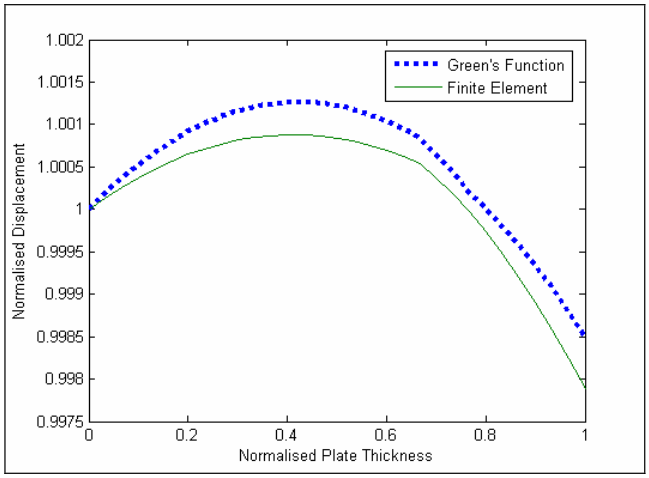

Figure 7. Anti-Symmetrical Displacement Profile

Derivative discontinuities can be seen at the interface between the three materials. The change in material induces a change in the acoustic wave propagation. Figure 7 was obtained using 31 equally spaced nodes through the device depth, with a slightly different layer configuration. In this case, the FPW device consisted of 2.0 µm of Si_3N_4, 0.3 µm of Al followed by 0.7 µm layer of ZnO. Figure 7, has been normalized to the device depth, with the mid-plane of the structure at 0.5.

VII. Conclusions and Future Work

This paper has presented a two dimensional FE model of a FPW device. The model has shown good agreement with a more computationally efficient method based on a Green's function analysis.

Future development will include the mass loading effect of the electrodes as well as the device response due to liquid loading. Fluid analysis will be performed using ANSYS in two phases. It will be necessary to consider the FPW first, and then relate this to the liquid analysis using FLOWTRAN. It is also intended to perform a three-dimensional analysis of a FPW device to calculate electrical parameters such as admittance and susceptence. Work is currently progressing to fabricate such a FPW device to confirm the findings of the numerical analysis.

Acknowledgment

The authors would like to thank CRC for microTechnology for their financial assistance.

References

[1] S. W. Wenzel and R. M. White, "Silicon-based ultrasonic Lamb-Wave multisensors", Solid-State Sensor and Actuator Workshop, 1988. Technical Digest., IEEE , June 1988. pp 27-30.

[2] M. Vellekoop, "Acoustic wave sensors and their technology", Ultrasonics, vol 36, Issues 1-5, February 1998, Pages 7-14

[3] B.A. Auld, "Acoustic Fields and Waves In Solids", Krieger Publishing Company, vol 2, 1990.

[4] Ansys Inc, "ANSYS 7.0 Documentation", SAS IP, 2002

[5] S. J. Ippolito, K. Kalantar-zadeh, D. A. Powell and Wojtek Wlodarski, "A 3-Dimensional finite element approach for simulating acoustic wave propagation in layered SAW devices", Ultrasonics, 2003 IEEE Symposium on ,vol 1 , Oct. 2003 , pp 303 - 306

[6] E. L. Adler, "Bulk and Surface Acoustic Waves in Anisotropic Solids", article in "Advances in Surface Acoustic wave Technology – Systems and Applications", vol 1, World Scientific Publishing Company, 2000.

[7] A. R. Baghai-Wadji, O.Männer and R. Ganß-Puchstein, "Analysis and measurement of transducer end radiation in SAW filters on strongly coupled substrates", IEEE Transactions on Microwave Theory and Techniques, vol 37, no. 1, 1989, pp 150 – 158.

[8] D. P. Morgan, "Quasi-Static analysis of generalized SAW transducers using the Green's function method", IEEE Transactions on Sonics and Ultrasonics, vol SU-27, 1980, pp 111 – 123.

[9] R. F. Milsom, N.H.C. Reilly and M. Redwood, "Analysis of genereration and detection of surface and bulk acoustic waves by Interdigital Transducers", IEEE Transactions on Sonics and Uiltrasonics, vol. SU-24, 1977, pp 147 - 166